Copper resistance is essential for virulence of *Mycobacterium tuberculosis*

Frank Wolschendorf[a], David Ackart[b], Tej B. Shrestha[c], Laurel Hascall-Dove[b], Scott Nolan[d], Gyanu Lamichhane[d], Ying Wang[a], Stefan H. Bossmann[c], Randall J. Basaraba[b], and Michael Niederweis[a,1]

[a]Department of Microbiology, University of Alabama at Birmingham, Birmingham, AL 35294; [b]Department of Microbiology, Immunology, and Pathology, Colorado State University, Fort Collins, CO 80523-1619; [c]Department of Chemistry, Kansas State University, Manhattan, KS 66506-0401; and [d]Tuberculosis Animal Research and Gene Evaluation Taskforce, The Johns Hopkins University School of Medicine, Baltimore, MD 21231

Edited by Emil C. Gotschlich, The Rockefeller University, New York, NY, and approved December 6, 2010 (received for review June 30, 2010)

Copper (Cu) is essential for many biological processes, but is toxic when present in excessive amounts. In this study, we provide evidence that Cu plays a crucial role in controlling tuberculosis. A *Mycobacterium tuberculosis* (*Mtb*) mutant lacking the outer membrane channel protein Rv1698 accumulated 100-fold more Cu and was more susceptible to Cu toxicity than WT *Mtb*. Similar phenotypes were observed for a *M. smegmatis* mutant lacking the homolog Ms3747, demonstrating that these mycobacterial copper transport proteins B (MctB) are essential for Cu resistance and maintenance of low intracellular Cu levels. Guinea pigs responded to infection with *Mtb* by increasing the Cu concentration in lung lesions. Loss of MctB resulted in a 1,000- and 100-fold reduced bacterial burden in lungs and lymph nodes, respectively, in guinea pigs infected with *Mtb*. In mice, the persistence defect of the *Mtb mctB* mutant was exacerbated by the addition of Cu to the diet. These experiments provide evidence that Cu is used by the mammalian host to control *Mtb* infection and that Cu resistance mechanisms are crucial for *Mtb* virulence. Importantly, *Mtb* is much more susceptible to Cu than other bacteria and is killed in vitro by Cu concentrations lower than those found in phagosomes of macrophages. Hence, this study reveals an Achilles heel of *Mtb* that might be a promising target for tuberculosis chemotherapy.

immune system | metal | accumulation

One of the most dangerous pathogens to mankind is *Mycobacterium tuberculosis* (*Mtb*). A key component of the immune response to *Mtb* is the IFN-γ–mediated activation of macrophages, resulting in efficient maturation of phagosomes with enhanced capacity to kill intracellular pathogens by using a range of hydrolytic enzymes, bactericidal peptides, and reactive oxygen and nitrogen intermediates (1). Copper (Cu) proteins are widely used for electron transfer reactions in the presence of oxygen because of the high redox potential of Cu(II)/Cu(I) (2). Hence, Cu is an essential nutrient for many bacteria, but it is also toxic because of the Cu(I)-catalyzed formation of hydroxyl radicals from hydrogen peroxide or other mechanisms (3). To avoid any free Cu ions cells use Cu-specific chaperones, storage proteins, and efflux systems (4). Early observations indicated that the toxicity of free Cu(I) in the presence of hydrogen peroxide may be used by the human immune system to fight bacterial pathogens (5, 6). Recent in vitro experiments with macrophages showed that IFN-γ–stimulated trafficking of the Cu transporter ATP7A to vesicles that fuse with phagosomes increasing their Cu content and their bactericidal activity against *Escherichia coli* (7). The first indication that the immune system might use Cu also to control growth of mycobacteria was provided by the finding that Cu concentrations are markedly increased within the phagosomal compartment of macrophages infected with *M. avium* (8).

Transcriptome analysis identified 30 Cu-responsive genes in *Mtb* (9), suggesting that *Mtb* faces critical concentrations of Cu during its life cycle. The *ctpV* gene (*rv0969*) is part of a Cu-induced operon controlled by the transcriptional regulator CsoR (10) and likely encodes a Cu-specific inner membrane efflux pump (9, 10). However, the *ctpV* mutant did not show a clear virulence defect in mice and guinea pigs (11). Further, *Mtb* produces the metallothionine MymT, a small protein that binds up to six Cu(I) ions and partially protects *Mtb* from Cu toxicity (12). The lack of MymT also did not reduce the virulence of *Mtb* in mice (12). These studies show that Cu resistance mechanisms exist in *Mtb*. However, it is unknown whether phagosomal Cu concentrations are sufficient to kill *Mtb in vivo* and how important Cu defense mechanisms are for virulence of *Mtb*.

Here, we present evidence that the outer membrane channel protein Rv1698 (13) is part of a Cu resistance mechanism that ensures low intracellular Cu levels in *Mtb* and protects the bacterium from the toxic effects of excess Cu. Importantly, we show that Rv1698 is required for full virulence of *Mtb* in guinea pigs and that guinea pigs respond to infections with *Mtb* by increasing Cu concentrations in lung lesions. This study provides experimental evidence that Cu resistance is crucial for survival of *Mtb* in animal hosts, establishes Cu as an antimycobacterial tool used by the immune system, and identifies a resistance mechanism by which excess Cu ions are limited within the bacterium.

Manuscript Text

To examine the physiological functions of the outer membrane channel protein Rv1698 of *Mtb* and its homolog in *M. smegmatis,* Ms3747, we constructed the *M. smegmatis* mutant ML77 lacking expression of the *ms3747* gene (*SI Appendix*, Fig. S1 *A* and *B*). Western blot experiments demonstrated the absence of the Ms3747 protein in detergent extracts of ML77 (Fig. 1*A*). ML77 exhibited a severe growth defect on Middlebrook 7H10 agar plates. This phenotype was restored by expression of *ms3747* or *rv1698* (*SI Appendix*, Fig. S2). Surprisingly, ML77 grew similarly to WT *M. smegmatis* SMR5 in Luria-Bertani (LB) medium, indicating that ML77 has no general growth defect, but rather might be more susceptible to a toxic compound present in Middlebrook 7H10 agar. Indeed, ML77 grew as well as WT *M. smegmatis* on plates made of 7H10 agar without added copper (Fig. 1*B*), but was impaired in the presence of 25 μM $CuSO_4$ (Fig. 1*B*), demonstrating that the lack of Ms3747 made *M. smegmatis* susceptible to copper. This phenotype was abolished by expression of either *ms3747* or *rv1698* (*SI Appendix*, Fig. S2), indicating that the susceptibility of ML77 to Cu was solely due to the lack of Ms3747 and that the *Mtb* homolog Rv1698 has a similar function.

Minimal inhibitory concentrations of 100 and 250 μg/mL $CuSO_4$ on 7H10 agar plates were determined for ML77 and WT *M. smegmatis*, respectively (*SI Appendix*, Fig. S3). Concentrations

Author contributions: F.W., G.L., S.H.B., R.J.B., and M.N. designed research; F.W., D.A., T.B.S., L.H.-D., S.N., and Y.W. performed research; F.W., D.A., T.B.S., G.L., S.H.B., R.J.B., and M.N. analyzed data; and R.J.B. and M.N. wrote the paper.

The authors declare no conflict of interest.

This article is a PNAS Direct Submission.

[1]To whom correspondence should be addressed. E-mail: mnieder@uab.edu.

This article contains supporting information online at www.pnas.org/lookup/suppl/doi:10.1073/pnas.1009261108/-/DCSupplemental.

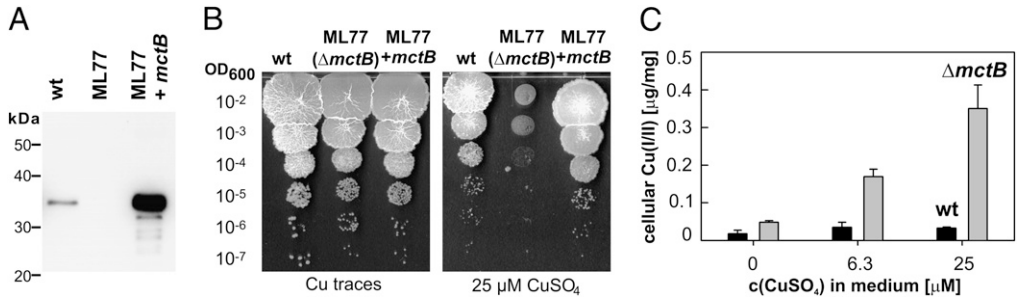

Fig. 1. MctB is required for copper resistance of and maintaining a low intracellular copper concentration in *M. smegmatis*. (*A*) Expression of *ms3747* in *M. smegmatis*. Proteins were extracted with 2% SDS from WT *M. smegmatis*, the *ms3747* mutant ML77, and ML77 complemented with the *ms3747* expression vector pML451. Proteins were detected in a Western blot by using the monoclonal antibody 5D1.23. (*B*) Serial dilutions of cultures of *M. smegmatis* SMR5 (WT), ML77 (Δ*mctB*), and ML77 complemented with *mctB* were spotted on 7H10 agar plates without or with CuSO4 at a concentration of 25 μM. (*C*) *M. smegmatis* SMR5 (black bars) and the Δ*ms3747* mutant ML77 (gray bars) were grown in self-made Middlebrook 7H9 medium with 0, 6.3, or 25 μM $CuSO_4$. Samples were taken after growth for 36 h. Copper was determined by measuring the absorption of the Cu(II)–dithizone complex at 553 nm.

of 200 μM $AgNO_3$ also impaired the growth of ML77 compared with WT *M. smegmatis*, whereas $HgCl_2$ and $CoCl_2$ had no effect (*SI Appendix*, Fig. S4). These results showed that Ms3747 is required for normal growth of *M. smegmatis* in the presence of elevated concentrations of Cu(II) and Ag(I) ions.

ML77 in Middlebrook 7H9 liquid cultures formed large clumps, in contrast to the parent WT strain (*SI Appendix*, Fig. S5). A similar phenotype is often caused by increased cell surface hydrophobicity. However, a complete lipid analysis did not reveal any differences between WT *M. smegmatis* and ML77. In addition, surface hydrophobicity was not changed as determined by Congo Red adsorption. These results suggest a specific defect of ML77 grown in liquid 7H9 medium as opposed to a general defect in membrane architecture or lipid properties.

To examine how Ms3747 contributes to Cu resistance of *M. smegmatis,* WT *M. smegmatis*, and the *ms3747* mutant ML77 were grown in the absence or presence of 6.3 or 25 μM Cu in self-made 7H9 medium, and the Cu content of cell lysates was determined by measuring Cu(II)-specific absorption changes of dithizone (14). The Cu content of WT *M. smegmatis* did not change regardless of the external Cu(II) concentration. By contrast, the Cu content of ML77 increased by 11-fold at 25 μM external Cu(II) (Fig. 1*C*). These results show that Ms3747 is involved in maintaining low, homeostatic levels of intracellular copper.

Complementation of the Cu sensitivity of the *ms3747* mutant by *rv1698* and *ms3747* (*SI Appendix*, Fig. S2), the channel activity of Rv1698 in vitro (13), and the fact that outer membrane channel proteins are involved in transport processes indicate that these proteins are involved in transport of copper. Efflux is a known Cu resistance mechanism in other bacteria (15). Hence, we propose to name these proteins MctB (mycobacterial Cu transport protein B).

To examine the function of *mctB* in *Mtb*, we constructed a mutant in a similar manner as done for *M. smegmatis* (Fig. 2*A*). The unmarked *mctB* mutant *Mtb* ML256 was confirmed by specific restriction digests (*SI Appendix*, Fig. S6) and sequencing of a PCR fragment amplified from chromosomal DNA. To obtain an MctB-specific antibody, hybridomas were generated from B cells harvested from mice immunized with recombinant *Mtb* MctB protein purified from *E. coli*. The monoclonal antibody 5D1.23 was the only antibody that recognized the MctB proteins from both *Mtb* and *M. smegmatis*. A Western blot using the 5D1.23 antibody showed that *mctB* is expressed in *Mtb* H37Rv grown in Middlebrook 7H9 medium, but absent in ML256 (Fig. 2*B*). Expression

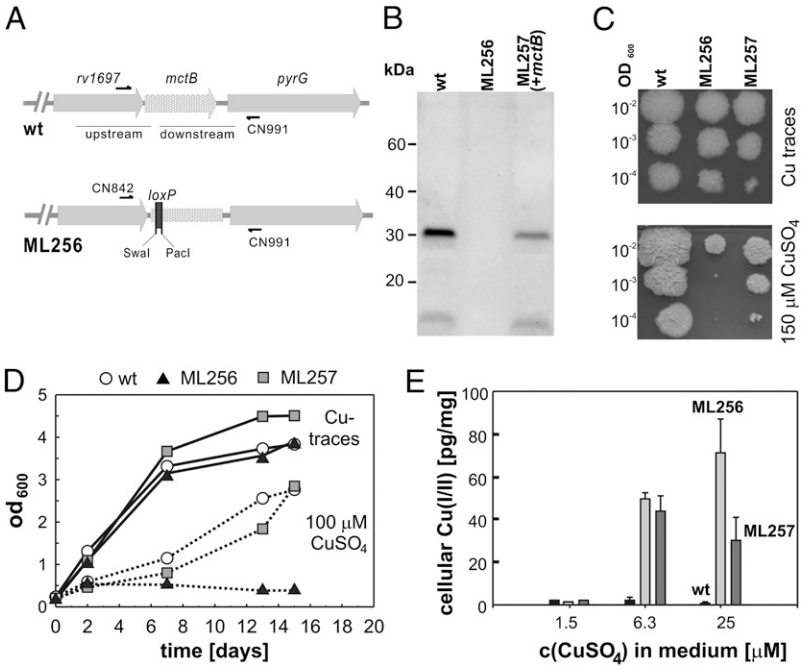

Fig. 2. MctB is required for copper resistance and maintenance of a low intracellular copper concentration in *M. tuberculosis*. (*A*) Schematic representation of the chromosomal *rv1698* region of *M. tuberculosis* H37Rv (WT). A fragment of 39 bp was replaced by the 45-bp *loxP* site in the 5′ part of the gene introducing stop codons in all three reading frames to construct the *rv1698* deletion mutant ML256 by homologous recombination. The genes are drawn to scale. (*B*) Expression of *mctB* in *Mtb*. Proteins were extracted with 2% SDS from WT *Mtb* and the *mctB* mutant ML256. ML257 is an ML256 derivative carrying the integrative *mctB* expression vector pML955. Proteins were detected in a Western blot by using the MctB-specific monoclonal antibody 5D1.23. (*C*) Copper susceptibility. Serial dilutions of log-phase cultures of *Mtb* H37Rv (WT), ML256 (Δ*mctB*), and ML257 (+*mctB*) were spotted on 7H11/OADC agar without or with $CuSO_4$ at a concentration of 150 μM. (*D*) Growth defect of *Mtb* Δ*mctB* mutant. *Mtb* WT, the Δ*mctB* mutant ML256, and the complemented mutant ML257 were grown in 7H10 medium supplemented with peptone (1 g/L) with or without 100 μM $CuSO_4$. The optical density at 600 nm was measured at the indicated time points. (*E*) *Mtb* (black bars), the Δ*mctB* mutant ML256 (light gray bars), and the complemented mutant ML257 (dark gray bars) were grown in minimal medium with 0.8, 6.3, or 25 μM $CuSO_4$. Copper was determined by measuring the absorption of the Cu(II)-dithizone complex at 553 nm.

of $mctB_{Mtb}$ was restored by integration of the plasmid pML955 (*SI Appendix*, Table S2) at the *attB* site of mycobacteriophage L5 (Fig. 2*B*). No growth difference was observed for WT *Mtb*, ML256 (Δ*mctB*), and ML257 (Δ*mctB*, $attB_{L5}$::$mctB_{Mtb}$) on 7H11 agar plates with Cu traces (Fig. 2*C*), demonstrating that the lack of *mctB* does not cause a general growth defect in *Mtb*. However, in the presence of 150 μM $CuSO_4$, the *mctB* mutant ML256 showed a severe growth defect in contrast to WT *Mtb* (Fig. 2*C*). Growth of ML256 in the presence of $CuSO_4$ was partially restored by expression of $mctB_{Mtb}$ (Fig. 2*C*). This finding is consistent with the sixfold lower $MctB_{Mtb}$ protein level compared with WT *Mtb* as determined by quantification of a Western blot of protein extracts (Fig. 2*B*). Growth inhibition of the *mctB* mutant ML256 by Cu was even more pronounced in liquid medium. Without Cu, all strains grew at a similar rate, whereas the *mctB* mutant did not grow in the presence of 100 μM $CuSO_4$ in contrast to WT *Mtb* and the complemented mutant (Fig. 2*D*).

To accurately assess the susceptibility of *Mtb* to copper, it was necessary to avoid albumin in the medium, which is known to sequester Cu ions in large quantities (3). Indeed, the high Cu susceptibility of the *M. smegmatis mctB* mutant ML77 was completely overcome by addition of either albumin or OADC, an albumin-containing supplement in media for *Mtb*. Therefore, *Mtb* was grown in Hartmans-de Bont minimal medium (HdB) and plated on HdB agar plates containing different $CuSO_4$ concentrations (*SI Appendix*, Fig. S7). All *Mtb* strains grew normally at 1.5 μM $CuSO_4$. No growth was observed ≥24 μM $CuSO_4$, indicating that *Mtb* is more susceptible to Cu than *M. smegmatis*, which tolerated up to 100 μM Cu (*SI Appendix*, Fig. S3). Serial dilutions of cultures of *Mtb* H37Rv and of ML256 (Δ*mctB*) on 7H11/OADC plates showed that the addition of Cu(I)-chelating bathocuproine disulfonate (BCS) restored growth of WT *Mtb* and of the *mctB* mutant ML256 in the presence of 150 μM $CuSO_4$ (*SI Appendix*, Fig. S8), indicating that Cu(I) is the Cu-species toxic for *Mtb*, which is consistent with previous findings (12).

The amount of Cu accumulated by WT *Mtb* was consistently low and independent of external $CuSO_4$ concentrations as determined by the dithizone assay (Fig. 2*E*). By contrast, the Cu content of ML256 increased drastically by 100-fold with increasing $CuSO_4$ concentrations in the medium (Fig. 2*E*), demonstrating the essential role of MctB for maintaining a low Cu concentration in *Mtb*. This effect was complemented in ML257 by expression of *mctB*, indicating that no other mutation caused the Cu sensitivity of the *mctB* mutant. However, this complementation was only partial, probably due to the lower expression of the integrated *mctB* gene in ML257 in contrast to the full complementation when *mctB* was expressed on a higher level in the *M. smegmatis* mutant ML77 (Fig. 1*B*).

It should be noted that the intracellular Cu concentration in *Mtb* was >10,000-fold lower than that measured in *M. smegmatis*. The decreased level of copper in *Mtb* might be due to its slower growth, which probably requires much less copper, compared to *M. smegmatis*. Taken together, these results demonstrate that MctB is required by *Mtb* and *M. smegmatis* for Cu resistance and for maintaining low intracellular Cu levels.

To examine the specificity of MctB, we tested the susceptibility of the *Mtb mctB* mutant to other physiologically relevant transition metals such as Fe(III), Zn(II), Mn(II), and Ni(II) under similar conditions as for Cu(II). The chosen concentrations were at or above the concentrations previously determined in mycobacteria-containing phagosomes of infected macrophages (8). With the exception of copper, none of the tested metal ions impaired growth of the *mctB* mutant (*SI Appendix*, Fig. S9*A*). By contrast, growth of the *mctB* mutant was reduced by Cu(II) by two orders of magnitude, demonstrating that *mctB* is Cu-specific (*SI Appendix*, Fig. S9*A*).

Expression of the *mymT* gene encoding a copper-binding metallothionein of *Mtb* was induced up to 1,000-fold in response to copper and nitric oxide (12). Thus, an alternative explanation for the increase the Cu susceptibility of the *mctB* mutant ML256 could be that the lack of MctB might indirectly reduce *mymT* expression. However, a dot blot with a MymT-specific antibody revealed that *mymT* expression was strongly induced to similar levels in all three strains in the presence of 100 μM $CuSO_4$ (*SI Appendix*, Fig. S10). In addition, agar dilution experiments also showed that the *Mtb mctB* mutant was not more susceptible to compounds that generate nitric oxide (*SI Appendix*, Fig. S9*C*), hydrogen peroxide (*SI Appendix*, Fig. S9*D*), or SDS (*SI Appendix*, Fig. S9*B*). Taken together, these experiments showed that *mctB* deletion does not cause a pleiotropic defect that would make *Mtb* more susceptible to reactive nitrogen and oxygen intermediates or cell-wall active compounds such as SDS, but rather it is the increased accumulation that makes the *Mtb mctB* mutant more susceptible to copper.

To assess the role of copper resistance in general and of MctB in the virulence of *Mtb* in particular, BALB/c mice were infected with aerosols containing *Mtb* H37Rv, the *mctB* mutant ML256, and the complemented mutant ML257. In the third week after infection, 10-fold fewer ML256 bacilli were detected compared with WT *Mtb* (*SI Appendix*, Fig. S11*A*). However, expression of *mctB* did not restore full virulence in the strain ML257, probably due to the sixfold lower MctB levels in ML257 compared with WT *Mtb* (Fig. 2*B*) and/or significantly lower initial inocula for the ML257-infected mice. Importantly, survival of the *Mtb mctB* mutant ML256 in the lungs of mice was severely compromised, resulting in a 100-fold decrease in bacterial burden compared with WT *Mtb*, in mice that were fed $CuSO_4$ in their diet (*SI Appendix*, Fig. S11*B*). These observations indicate that the impaired survival of ML256 is a Cu-specific effect. Further support for the beneficial effect of Cu for mice infected with *Mtb* was provided by histopathology. Lung sections of mice infected with both WT *Mtb* and ML256 showed significantly fewer lymphocytic infiltrates and fewer overall lesions when the mice were fed additional Cu (*SI Appendix*, Fig. S12).

The finding that hypoxia induces Cu transport into macrophages and, thereby, increases their bactericidal potential (7, 16) and the fact that hypoxia does not exist in *Mtb*-infected mice (17) indicate that mice might not be a good animal model to examine the role of *MctB* in virulence of *Mtb*. By contrast, in guinea pigs, *Mtb* induces formation of discrete, granulomatous lesions with central necrosis and dystrophic mineralization similar to those of humans. We considered formation of these hypoxic granulomas as important for assessing the role of Cu in the mammalian immune system, because oxygen limitation was shown to stimulate Cu delivery to phagosomes containing bacteria (16). To examine the role of Cu in the response of guinea pigs to infection with *Mtb*, we isolated, microdissected and pooled granulomas from lungs of guinea pigs infected with WT *Mtb* H37Rv and analyzed trace minerals by flame atomic absorption spectrophotometry as described (18). The Cu concentration in isolated primary granulomas, where bacilli are concentrated, was significantly increased compared with unaffected lung parenchyma (Fig. 3*A*). These data show that *Mtb* is exposed to increased concentrations of Cu in vivo in lung lesions of guinea pigs and indicate that guinea pigs are a better animal model to evaluate the role of Cu resistance for virulence of *Mtb*. Therefore, guinea pigs were infected by low-dose aerosols with WT H37Rv, the isogenic Δ*mctB* mutant (ML256), or the complemented mutant ML257. Thirty days after infection, the bacterial burden of the Δ*mctB* mutant ML256 in the lungs of infected guinea pigs was reduced by >1,000-fold compared with WT *Mtb*. Low-level expression of *mctB* in ML257 partially complemented this virulence defect (Fig. 3*B*). The Δ*mctB* mutant was also significantly impaired in dissemination from the lung to the draining lymph nodes compared with the WT and complemented (ML257) strains, but was not affected in its ability to disseminate from the lung to the spleen (Fig. 3*B*). Despite its strong virulence defect, the Δ*mctB* mutant ML256 retained the ability to incite characteristic inflammatory lesions in the lung, lymph nodes and spleens of infected guinea pigs. Further, photomicrographs of representative lungs, lymph nodes, and spleens for ML256, ML257, and WT *Mtb* H37Rv show characteristic granulomatous inflammatory foci with central lesion necrosis (*SI Appendix*, Fig. S13, Fig. S14, and Fig. S15), indicating

that the attenuation of the Δ*mctB* mutant did not significantly alter the host response compared with WT *Mtb*. Taken together these data show that the loss of MctB caused a drastic virulence defect of *Mtb* in guinea pigs, which is primarily due to a much lower bacterial burden in the lungs.

Discussion

MctB (Rv1698, Ms3747) was discovered as an outer membrane channel protein with no homologs of known function (13). In this study, we show that MctB is required to maintain a nontoxic level of intracellular Cu in mycobacteria, implying that MctB is involved in Cu efflux. Support for this hypothesis is provided by the finding that *mctB* mutants are more susceptible to copper in contrast to porin mutants, which are typically more resistant to the transported solutes (19). Functionally similar proteins are known in Gram-negative bacteria. For example, the Cus efflux system is required for efficient Cu resistance by *E. coli* and consists of the inner membrane pump CusA, the outer membrane channel CusC, and the periplasmic membrane fusion protein CusB (20). Our finding that Ms3747 is required for resistance of *M. smegmatis* to Cu(I) and Ag(I) indicates that the main substrate of this efflux system is cytotoxic Cu(I) ions. Interaction of MctB with the putative Cu efflux pump CtpV (9) could provide the ion specificity and the energy for efflux against the concentration gradient and, hence, would explain the surprising specificity of the MctB pore for Cu(I) and Ag(I) despite its large single channel conductance of 4.3 nS (13). This principle is demonstrated by the tripartite metal and drug efflux systems in Gram-negative bacteria (21).

The minimal inhibitory concentration of Cu for *Mtb* is <24 μM (*SI Appendix*, Fig. S7), which is much lower than that of *E. coli* (≈3 mM) or of other bacteria (20). In addition, Cu appears to be bactericidal for *Mtb* (9) in contrast to *M. smegmatis*, whose growth is strongly delayed by high Cu concentrations (*SI Appendix*, Fig. S3), but eventually recovers to yield normal colony sizes. Importantly, Cu concentrations in the range of the minimal inhibitory concentration for *Mtb* have been determined in phagosomes of macrophages infected with *M. avium* and *Mtb* by microprobe X-ray fluorescence (8). Thus, Cu concentrations lethal to *Mtb* appear to exist in the phagosome of activated macrophages. These findings indicate that macrophages use Cu as a defensive weapon against *Mtb* and possibly other bacterial pathogens. Indeed, the Cu transporter ATP7A was required for full bactericidal activity of macrophages against *E. coli* (7). Interestingly, both IFN-γ and hypoxia stimulate trafficking of the Cu transporter ATP7A from the Golgi to phagosomes (7, 16). Hypoxia also increased expression of the Cu importer CTR1 (Fig. 4) and, hence, stimulated Cu uptake by macrophages resulting in increased Cu delivery to the ATP7A Cu transporter, in trafficking of ATP7A to cytoplasmic vesicles, and decreased expression of Cu-containing enzymes (16). Thus, upon stimulation with IFN-γ and under hypoxic conditions, both of which are crucial responses of the immune system to infection with *Mtb* (17, 22), macrophages increase Cu uptake and redirect the available Cu to ATP7A for delivery into phagosomes (Fig. 4).

Considering the compelling in vitro data that Cu plays a key role in the bactericidal activity of macrophages, it is tempting to speculate that Cu resistance mechanisms of *Mtb* are important for bacterial virulence. However, previous studies showed only a modest increase in Cu susceptibility of *Mtb* in the absence of the copper-binding metallothionein MymT (12) and the putative inner membrane CtpV (11) and no or only a minor virulence defect in mice or guinea pigs. By contrast, the survival of the Δ*mctB* mutant ML256 in the lungs of guinea pigs was strongly impaired as compared with WT *Mtb*, resulting in a 1,000- and 100-fold reduced bacterial burden in lungs and lymph nodes (Fig. 3*B*). These results indicate that the role of MctB in Cu resistance of *Mtb* is less redundant than that of MymT or CtpV. Taken together, the

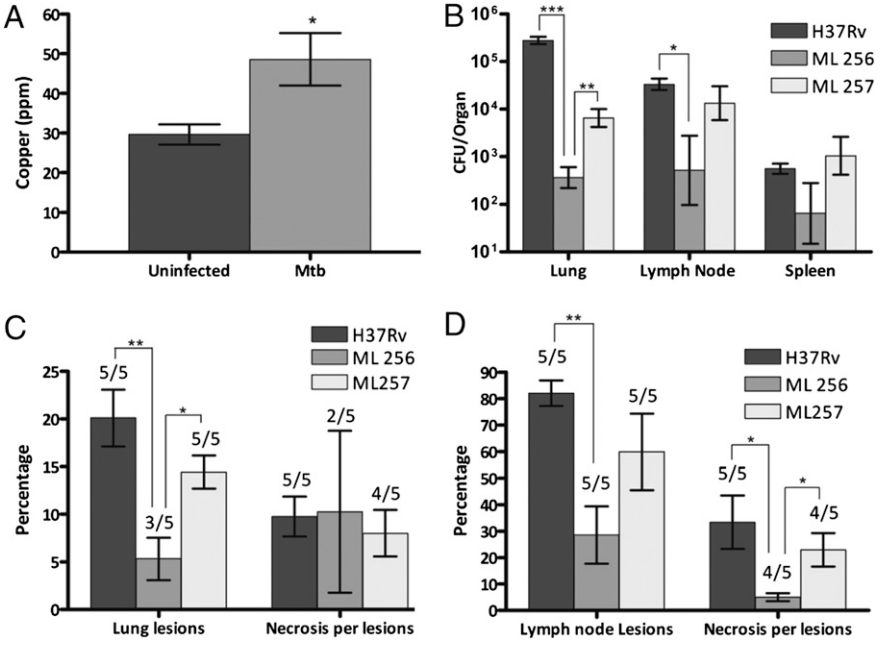

Fig. 3. MctB-mediated copper resistance is required for virulence of *M. tuberculosis* in guinea pigs. (*A*) Cu concentrations in granulomatous lesions from guinea pigs infected with *Mtb* H37Rv. Tissue Cu was measured by atomic absorption spectroscopy in homogenates of lung parenchyma of five uninfected guinea pigs, and pooled primary granulomas were isolated by microdissection from lungs of five infected guinea pigs. *$P \leq 0.05$. (*B–D*) Guinea pigs were infected with *Mtb* WT H37Rv (dark gray bars), the Δ*mctB* mutant ML256 (medium gray bars), and the complemented mutant ML257 (light gray bars). (*B*) The bacterial burden in lung, lymph node, and spleen was determined from tissue homogenates from guinea pigs 30 d after infection. *$P \leq 0.05$, **$P \leq 0.01$, ***$P \leq 0.001$; number of infected animals per data point: $n = 5$. (*C*) Lung lesions were quantified from the area of total lung parenchyma affected by granulomatous inflammation. Data represents the mean percentage of affected lung for each treatment group or the mean percent area of lesions with necrosis. *$P \leq 0.05$, **$P \leq 0.01$; $n = 5$. (*D*) Lymph node lesions were quantified from the area of total lymph node parenchyma affected by granulomatous inflammation. Data represents the mean percentage of affected lymph node for each treatment group or the mean percent area of lesions with necrosis. *$P \leq 0.05$, **$P \leq 0.01$; $n = 5$.

increase of copper in the *Mtb*-containing granulomas of guinea pigs and the infection experiments in this study strongly indicate that Cu is used by mammalian immune systems to control growth of *Mtb* and demonstrate that, in turn, Cu resistance mechanisms are crucial for virulence of *Mtb*. The smaller virulence defect of the Δ*mctB* mutant in mice is likely due to the fact that mice do not form hypoxic granulomas (17). Because granuloma formation is a hallmark of the human immune response to infections with *Mtb* (22, 23), these findings also indicate that Cu might play a crucial role in humans infected with *Mtb*.

This study demonstrates that Cu resistance is crucial for survival of *Mtb* in the mammalian host. Based on the findings of this study, we propose the following model of how the mammalian immune system might control *Mtb* by using a Cu-dependent mechanism (Fig. 4). Macrophages generate an oxidative burst against intracellular pathogens that includes the release of hydrogen peroxide (24). Hydrogen peroxide, in contrast to other reactive oxygen species, can diffuse well through membranes (25). The immune system responds to infection with *Mtb* by secretion of IFN-γ by $CD4^+$-T cells (26) that, in addition to other reactions, stimulates expression of the high-affinity copper importer CTR1 in macrophages (7). Hypoxic conditions, a hallmark of granulomas formed in humans after lung infection with *Mtb*, induce *CTR1* expression and the chaperone ATOX1 and the copper transporter ATP7A (16) redirect Cu traffic to the *Mtb*-containing phagosome. Higher concentrations of Cu increases the formation of toxic hydroxyl radicals from hydrogen peroxide, a reaction that is catalyzed by Cu(I) (3). To protect itself from toxic effects of free Cu (I) *Mtb* utilizes at least two resistance mechanisms (Fig. 4), which might be partially redundant as observed for *E. coli* (15): sequestration of Cu by the metallothionein MymT (12) and probably efflux by the inner membrane transporter CtpV (11). The channel protein MctB might interact with CtpV to enable efflux of Cu across the outer membrane of *Mtb.* The observation that MctB is required for virulence of *Mtb* in guinea pigs suggests that the binding capacity of MymT might be eventually overwhelmed in the absence of MctB.

This study revealed an alternative target for tuberculosis chemotherapy, in which MctB might be inactivated by a drug and, thereby, makes *Mtb* more vulnerable to Cu ions used by macrophages to kill *Mtb*. Such an approach may lead to a new class of anti-infectives that could sensitize pathogens to host immune responses by inhibiting bacterial defense mechanisms as recently described by Carl Nathan and colleagues (27). Targeting MctB might be a promising strategy because the surface accessibility of MctB (28) may enable putative inhibitors to reach its target directly without the need to cross the notoriously impermeable outer membrane of *Mtb*, a major determinant of intrinsic drug resistance (29).

Materials and Methods

Bacterial Strains and Growth Conditions. The strains used in this study are listed in *SI Appendix*, Table S3. Media and growth conditions are described in *SI Appendix*.

Plasmid Construction. Construction of the plasmids is described in *SI Appendix*, Table S2.

Construction of the ΔmctB Mutants of *M. smegmatis* and Mtb. The *mctB* mutants of *M. smegmatis* (*ms3747*) and *Mtb* (*rv1698*) were constructed by using a two-step selection strategy as described in *SI Appendix*.

Preparation and Analysis of Protein Extracts. An overnight culture of *M. smegmatis* grown in self-made 7H9 (7H9sm) medium was used to inoculate 7H9sm medium with or without copper. Proteins were extracted from *M. smegmatis* by using 2% SDS in PBS at 40 °C as described (13). Proteins were analyzed in Western blots by using specific antibodies raised against MctB (5D1.23), MymT (kindly provided by Ben Gold), and horseradish peroxidase-coupled anti-mouse or anti-rabbit secondary antibodies as described (30). For further details, see *SI Appendix*.

Metal Susceptibility Assays. To determine the susceptibility of WT *M. smegmatis* and ML77 to copper, self-made 7H10 (7H10sm) plates were prepared containing different concentrations of $CuSO_4$. The strains were grown in 7H9sm medium without Cu overnight. The cultures were filtered through a 5-μm filter to obtain single-cell suspensions. Plates with appropriate dilutions were incubated at 37 °C. The susceptibility of *M. smegmatis* to silver, mercury, and cobalt was measured on Mueller-Hinton agar plates to prevent formation of water-insoluble salts. The concentration of $AgNO_3$, HgCl, and $CoCl_2$ in these plates was 1.6, 8, 40, and 200 μM. Copper sulfate was used as a control. *Mtb* was grown in 7H9/OADC medium for 7 d. Appropriate dilutions were dropped on 7H11 agar plates containing $CuSO_4$, ammonium iron (III) citrate, $MnCl_2$, $ZnCl_2$, and $NiCl_2$ at the indicated concentrations.

Copper Accumulation. Precultures of *M. smegmatis* strains were grown in 7H9sm medium without copper. Then, three cultures of each *M. smegmatis* strain were inoculated in 7H9sm medium with 0, 6.3, or 25 μM $CuSO_4$ and shaken at 37 °C. Samples were taken 36 h after inoculation. Precultures of each *Mtb* strain were grown in HdB medium (30 mL) with 0.8 μM $CuSO_4$ and

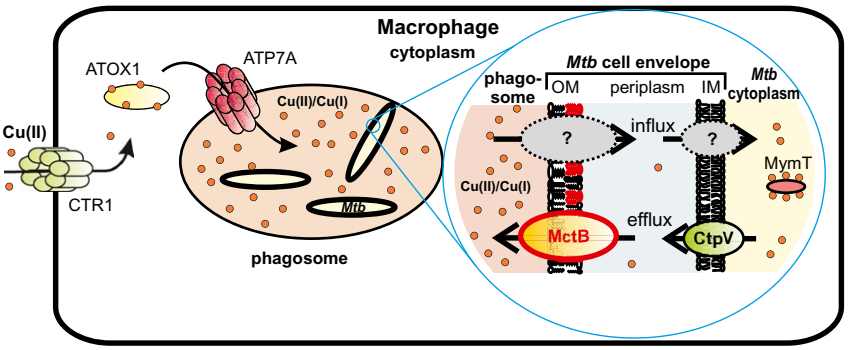

Fig. 4. Role of copper in bactericidal activity of macrophages and model of copper-resistance mechanisms of *M. tuberculosis*. Cu(II) is taken up across the plasma membrane of macrophages by the high-affinity Cu transporter Ctr1 (32). The Cu-chaperon Atox1 is a cytoplasmic Cu-binding and -transport protein that interacts with the Cu(II)-transporting ATPase Atp7A (33). In macrophages stimulated by IFN-γ or by hypoxia, cytoplasmic vesicles that contain Atp7A fuse with phagosomes (16). As a consequence, Cu is pumped into the phagosome, which contributes to its bactericidal activity (7). MctB is a pore-forming protein located in the outer membrane (OM) of *Mtb* (13) and prevents the accumulation of Cu within the mycobacterial cell probably by efflux of cuprous ions. Another important component of Cu homeostasis in *Mtb* is the cytoplasmic Cu-binding metallothionein MymT (12). The inner membrane (IM) transporter CtpV might be a Cu efflux protein (9, 11).

used to inoculate triplicate cultures for each Cu concentration by using the same medium (25 mL). All *Mtb* cultures were incubated for 8 d at 37 °C before the $CuSO_4$ concentration was either kept at 0.8 μM or adjusted to 6.3 or 25 μM. Samples were taken after 10 d. Generally, samples were centrifuged at 3,250 × *g* and washed twice in the appropriate medium without added Cu. For *Mtb*, the washed pellets were resuspended in 0.5 mL of ultrapure water and boiled for 1 h to inactivate *Mtb*. All samples were dried at 60 °C overnight under vacuum. Dried pellets were suspended in 600 μL of H_2O and sonicated for 20 min in a sonicator bath. The Cu content of the cells was analyzed by using the photometric dithizone assay as published (14). For details, see *SI Appendix*.

Experimental Infections in Mice. A preliminary Cu tolerance study was performed in which three groups of BALB/c mice (Charles River) were given water ad libitum containing 118 mg/L, 1180 mg/L, or 11.8 g/L Cu sulfate pentahydrate (Sigma). The mice were monitored for 2 wk. A concentration of 118 mg/L Cu sulfate pentahydrate did not cause any signs of distress in mice and was chosen for further experiments.

Midlog phase cultures of WT *Mtb*, the *mctB* mutant ML256, and the complemented mutant ML257 were diluted to $OD_{600} \approx 0.08$ to implant 500–1,000 bacilli in the lungs of mice by using a Middlebrook inhalation exposure system (Glas-Col). Eighty 4- to 6-wk-old BALB/c mice were infected with WT *Mtb* H37Rv or ML256, and 40 mice were infected with ML257. One day after infection, half of the infected mice were separated and given water ad libitum containing 118 mg/L Cu sulfate pentahydrate. Four mice from each group were weighed and killed at days 1, 7, 14, 28, 84, and 112 after infection to determine the number of bacilli in the lung and spleen. Mouse organs were aseptically removed, homogenized, and serially diluted. Appropriate dilutions were plated onto Middlebrook 7H11 agar plates to determine the colony-forming units. For histological analysis, representative tissue samples from each group were fixed in 10% formaldehyde, embedded in parraffin, sectioned, and stained with hematoxylin and eosin by using standard procedures.

Experimental Infections in Guinea Pigs. Guinea pigs were infected with *M. tuberculosis* strains H37Rv, ML 256, and ML257 by using an aerosol chamber, and determination of the bacterial load and histological analysis were done as described (31). Five animals were analyzed at each time point. For further details see *SI Appendix*. Grossly visible primary lung lesions for chemical analysis were dissected from paraformaldehyde fixed lungs of five guinea pigs infected with *Mtb*. Lungs were embedded in low melting point agar and sectioned into 3-mm slices. A subset of slices was selected by uniform random sampling. From those slices, individual primary lesions were dissected from lungs and pooled (>1 gram per animal). Equal quantities of samples collected in a similar fashion from paraformaldehyde-fixed lungs of five noninfected animals were used as negative controls. Pooled tissue samples from each animal were dried overnight in a drying oven at 85 °C, weighed to determine total dry weight per sample, and ashed overnight in a muffle furnace at 600 °C. The ashed samples were allowed to cool and then dissolved in nitric acid. The solutions were sonicated to complete dissolution. The resulting acid solution was diluted with deionized water for Cu analyses. Copper concentrations were determined via flame atomic absorption spectroscopy as described (19). The values for each of the five animals were averaged, and tissue concentrations were reported as parts per million of pooled samples on a dry weight basis.

ACKNOWLEDGMENTS. We thank Mamadou Daffe for lipid analysis, Adrie Steyn for providing the plasmids pCreSacB1 and pBS346; Ben Gold for providing MymT peptide and MymT-specific antibodies; and Jennifer Rowland, Jason Huff, and Ursula Niederweis for editing the manuscript. The Tuberculosis Animal Research and Gene Evaluation Taskforce program was supported by the National Institutes of Health Contract N01-AI30036. This work was supported by National Science Foundation Grant "Experimental Program to Stimulated Competitive Research" 4166 (to S.H.B.) and National Institutes of Health Grants AI083856 (to R.J.B.), AI083632 (to M.N.), and AI063432 (to M.N.).

1. Nathan C, Shiloh MU (2000) Reactive oxygen and nitrogen intermediates in the relationship between mammalian hosts and microbial pathogens. *Proc Natl Acad Sci USA* 97:8841–8848.
2. Crichton RR, Pierre JL (2001) Old iron, young copper: From Mars to Venus. *Biometals* 14:99–112.
3. Halliwell B, Gutteridge JM (1984) Oxygen toxicity, oxygen radicals, transition metals and disease. *Biochem J* 219:1–14.
4. Rae TD, Schmidt PJ, Pufahl RA, Culotta VC, O'Halloran TV (1999) Undetectable intracellular free copper: The requirement of a copper chaperone for superoxide dismutase. *Science* 284:805–808.
5. Prohaska JR, Lukasewycz OA (1981) Copper deficiency suppresses the immune response of mice. *Science* 213:559–561.
6. Newberne PM, Hunt CE, Young VR (1968) The role of diet and the reticuloendothelial system in the response of rats to Salmonella typhilmurium infection. *Br J Exp Pathol* 49:448–457.
7. White C, Lee J, Kambe T, Fritsche K, Petris MJ (2009) A role for the ATP7A copper-transporting ATPase in macrophage bactericidal activity. *J Biol Chem* 284: 33949–33956.
8. Wagner D, et al. (2005) Elemental analysis of Mycobacterium avium-, Mycobacterium tuberculosis-, and Mycobacterium smegmatis-containing phagosomes indicates pathogen-induced microenvironments within the host cell's endosomal system. *J Immunol* 174:1491–1500.
9. Ward SK, Hoye EA, Talaat AM (2008) The global responses of Mycobacterium tuberculosis to physiological levels of copper. *J Bacteriol* 190:2939–2946.
10. Liu T, et al. (2007) CsoR is a novel Mycobacterium tuberculosis copper-sensing transcriptional regulator. *Nat Chem Biol* 3:60–68.
11. Ward SK, Abomoelak B, Hoye EA, Steinberg H, Talaat AM (2010) CtpV: A putative copper exporter required for full virulence of Mycobacterium tuberculosis. *Mol Microbiol* 77:1096–1110.
12. Gold B, et al. (2008) Identification of a copper-binding metallothionein in pathogenic mycobacteria. *Nat Chem Biol* 4:609–616.
13. Siroy A, et al. (2008) Rv1698 of Mycobacterium tuberculosis represents a new class of channel-forming outer membrane proteins. *J Biol Chem* 283:17827–17837.
14. Kumar B, Singh HB, Katyal M, Sharma RL (1991) Spectrophotometric and derivative spectrophotometric determination of copper (II) with dithizone in aqueous phase. *Microchim Acta* 105:79–87.
15. Rensing C, Grass G (2003) Escherichia coli mechanisms of copper homeostasis in a changing environment. *FEMS Microbiol Rev* 27:197–213.
16. White C, et al. (2009) Copper transport into the secretory pathway is regulated by oxygen in macrophages. *J Cell Sci* 122:1315–1321.
17. Via LE, et al. (2008) Tuberculous granulomas are hypoxic in guinea pigs, rabbits, and nonhuman primates. *Infect Immun* 76:2333–2340.
18. Basaraba RJ, et al. (2008) Increased expression of host iron-binding proteins precedes iron accumulation and calcification of primary lung lesions in experimental tuberculosis in the guinea pig. *Tuberculosis (Edinb)* 88:69–79.
19. Nikaido H (2003) Molecular basis of bacterial outer membrane permeability revisited. *Microbiol Mol Biol Rev* 67:593–656.
20. Franke S, Grass G, Rensing C, Nies DH (2003) Molecular analysis of the copper-transporting efflux system CusCFBA of Escherichia coli. *J Bacteriol* 185:3804–3812.
21. Nies DH (2003) Efflux-mediated heavy metal resistance in prokaryotes. *FEMS Microbiol Rev* 27:313–339.
22. Russell DG (2007) Who puts the tubercle in tuberculosis? *Nat Rev Microbiol* 5:39–47.
23. Ulrichs T, Kaufmann SH (2006) New insights into the function of granulomas in human tuberculosis. *J Pathol* 208:261–269.
24. Miller RA, Britigan BE (1997) Role of oxidants in microbial pathophysiology. *Clin Microbiol Rev* 10:1–18.
25. Seaver LC, Imlay JA (2001) Hydrogen peroxide fluxes and compartmentalization inside growing Escherichia coli. *J Bacteriol* 183:7182–7189.
26. Flynn JL (2004) Immunology of tuberculosis and implications in vaccine development. *Tuberculosis (Edinb)* 84:93–101.
27. Nathan C, et al. (2008) A philosophy of anti-infectives as a guide in the search for new drugs for tuberculosis. *Tuberculosis (Edinb)* 88:S25–S33.
28. Song H, Sandie R, Wang Y, Andrade-Navarro MA, Niederweis M (2008) Identification of outer membrane proteins of Mycobacterium tuberculosis. *Tuberculosis (Edinb)* 88: 526–544.
29. Niederweis M, Danilchanka O, Huff J, Hoffmann C, Engelhardt H (2010) Mycobacterial outer membranes: In search of proteins. *Trends Microbiol* 18:109–116.
30. Stephan J, et al. (2005) The growth rate of Mycobacterium smegmatis depends on sufficient porin-mediated influx of nutrients. *Mol Microbiol* 58:714–730.
31. Ordway DJ, et al. (2010) Evaluation of standard chemotherapy in the guinea pig model of tuberculosis. *Antimicrob Agents Chemother* 54:1820–1833.
32. Prohaska JR, Gybina AA (2004) Intracellular copper transport in mammals. *J Nutr* 134: 1003–1006.
33. Hamza I, Prohaska J, Gitlin JD (2003) Essential role for Atox1 in the copper-mediated intracellular trafficking of the Menkes ATPase. *Proc Natl Acad Sci USA* 100:1215–1220.